

Bimetallic Compounds of *trans*-Cyclohexane-1,2-diamine-*NNN'*-tetra-acetate (cdta). Part 3.† Structural‡ and Magnetic Characterization of the Dinuclear $[M(OH_2)_5][M'(cdta)] \cdot H_2O$ ($M, M' = Ni, Ni; Mn, Ni; Mn, Cu; Co, Ni; \text{ or } Co, Cu$) and the Tetranuclear $[M(OH_2)_4][M'(cdta)(OH_2)] \cdot 4H_2O$ ($M, M' = Zn, Zn; Zn-Co; Co, Co; \text{ or } Mn, Co$) Complexes

Amparo Fuertes* and Carlos Miravittles

Institut de Ciència de Materials de Barcelona (C.S.I.C.), c/ Martí i Franquès, s/n. Aptdo 30102, 08028 Barcelona, Spain

Emilio Escrivá, Eugenio Coronado, and Daniel Beltrán*

Department de Química Inorgànica, Facultat de Ciències Químiques, Universitat de València (Estudi General), c/ Dr. Moliner, 50, 46100 Burjassot, València, Spain

Lilyane Padel

Département Science des Matériaux, E.H.I.C.S., 67008 Strasbourg Cedex, France

The crystal structures of the complexes $[Co(OH_2)_5][Cu(cdta)] \cdot H_2O$ (**5**), $[Zn(OH_2)_4][Zn(cdta)(OH_2)] \cdot 4H_2O$ (**6**), and $[Zn_{0.7}Co_{0.3}(OH_2)_4][Zn_{0.3}Co_{0.7}(cdta)(OH_2)] \cdot 4H_2O$ (**7**) (*cdta* = *trans*-cyclohexane-1,2-diamine-*NNN'*-tetra-acetate) have been determined by *X*-ray methods. They crystallize in space groups *Pbc*2₁, *P2₁/n*, and *P2₁/n* respectively. The respective unit-cell constants are: *a* = 10.878(5), 9.702(2), 9.731(9) Å; *b* = 11.167(5), 11.757(2), 11.783(2) Å; *c* = 17.446(14), 20.980(5), 21.031(9) Å; β = 90, 95.61(2), 95.40(6)°. The *Z* value is 4 for all three compounds. The structures were solved by direct methods and refined to final respective *R* values of 0.056, 0.098, and 0.041. The structure of (**5**) consists of dinuclear entities, constructed from cationic $[Co(OH_2)_5]^{2+}$ and anionic $[Cu(cdta)]^{2-}$ molecules which are linked through a bridging carboxylate group from the *cdta* ligand. In (**6**) and (**7**), the species $[M(2)(OH_2)_4]^{2+}$ and $[M(1)(cdta)(OH_2)]^{2-}$ [*M*(1), *M*(2) = Zn, Co], sharing two oxygen atoms from different carboxylate groups, alternate in order to form tetranuclear entities. Magnetic properties in the range 1–100 K of compound (**5**) and those of the derivatives $[Ni(OH_2)_5][Ni(cdta)] \cdot H_2O$ (**1**), $[Mn(OH_2)_5][Ni(cdta)] \cdot H_2O$ (**2**), $[Mn(OH_2)_5][Cu(cdta)] \cdot H_2O$ (**3**), $[Co(OH_2)_5][Ni(cdta)] \cdot H_2O$ (**4**), $[Co(OH_2)_4][Co(cdta)(OH_2)] \cdot 4H_2O$ (**8**), and $[Mn(OH_2)_4][Co(cdta)(OH_2)] \cdot 4H_2O$ (**9**) are discussed by assuming a Heisenberg or Ising exchange coupling between the two metal ions with distinct Landé factors and local distortion parameters. All the compounds show antiferromagnetic behaviour at low temperatures, with exchange coupling parameters ranging from –0.8 [(**5**)] to –8.8 cm^{–1} [(**4**)].

The major progress in magnetostructural chemistry in the past few years has been the systematic development of structurally ordered bimetallic compounds.¹ In this sense, the family of ethylenediamine-*NNN'*-tetra-acetate (*edta*) complexes $[M(OH_2)_4][M'(edta)] \cdot 2H_2O$ (*M* = Mg, Mn, Co, Zn, or Ni; *M'* = Co, Ni, Cu, or Zn) has been shown to be a very versatile structural support for investigating a wide variety of low-dimensional ferrimagnetic systems.^{2–6}

As a part of our studies in the search of new ordered bimetallic compounds we have approached the magnetostructural chemistry of bimetallic *trans*-cyclohexane-1,2-diamine-*NNN'*-tetra-acetate (*cdta*) complexes. Thus, five structural types have been found,^{7,8} namely: (i) type A, formed by the copper homometallic alternating chain $[Cu(OH_2)_4][Cu(cdta)]$;⁹ (ii) type B, formed by the dimeric complexes formulated as $[M(OH_2)_5][M'(cdta)] \cdot H_2O$ (*M, M'* = Zn, Cu; Ni, Cu; Co, Cu; Mn, Cu; Ni, Ni; Zn, Ni; Mn, Ni; Mg, Ni; Mg, Zn; or Co, Ni);¹⁰ (iii) type C, formed by the dimeric complex $[Cu(OH_2)_4][Ni(cdta)] \cdot 3H_2O$;¹¹ (iv) type D, formed by the family of tetrameric compounds $[M(OH_2)_4][M'(cdta)(OH_2)] \cdot 4H_2O$ (*M, M'* = Zn, Zn, Zn–Co, Mn, Co, or Co, Co); and (v) type

E, formed by the polymeric compounds $[M(OH_2)_4][M'(cdta)] \cdot 3H_2O$ (*M, M'* = Mn, Mn or Mn, Cd).¹²

In previous papers the structures of types A and C have been reported and their magnetic properties discussed by assuming an isotropic exchange coupling between the interacting ions.^{9,11} Here we report the crystal structures of the compounds $[Co(OH_2)_5][Cu(cdta)] \cdot H_2O$, $[Zn(OH_2)_4][Zn(cdta)(OH_2)] \cdot 4H_2O$, and $[Zn_{0.7}Co_{0.3}(OH_2)_4][Zn_{0.3}Co_{0.7}(cdta)(OH_2)] \cdot 4H_2O$ as representatives of types B and D and the magnetic properties of the derivatives belonging to these structural families. According to the electronic ground state of the interacting ions these properties are discussed by assuming Heisenberg or Ising exchange couplings between the two metal ions with distinct Landé factors and local distortion parameters.

Experimental

Preparation and Characterization of the Complexes.—All the compounds $[Ni(OH_2)_5][Ni(cdta)] \cdot H_2O$ (**1**), $[Mn(OH_2)_5][Ni(cdta)] \cdot H_2O$ (**2**), $[Mn(OH_2)_5][Cu(cdta)] \cdot H_2O$ (**3**), $[Co(OH_2)_5][Ni(cdta)] \cdot H_2O$ (**4**), $[Co(OH_2)_5][Cu(cdta)] \cdot H_2O$ (**5**), $[Zn(OH_2)_4][Zn(cdta)(OH_2)] \cdot 4H_2O$ (**6**), $[Zn_{0.7}Co_{0.3}(OH_2)_4][Zn_{0.3}Co_{0.7}(cdta)(OH_2)] \cdot 4H_2O$ (**7**), $[Co(OH_2)_4][Co(cdta)(OH_2)] \cdot 4H_2O$ (**8**), and $[Mn(OH_2)_4][Co(cdta)(OH_2)] \cdot 4H_2O$ (**9**) were prepared by the procedure described in ref. 8 and their composition confirmed by microanalysis. *X*-Ray powder

† Refs. 9 and 11 to be regarded as Parts 1 and 2 respectively.

‡ Supplementary data available: see Instructions for Authors, *J. Chem. Soc., Dalton Trans.*, 1989, Issue 1, pp. xvii–xx.

Table 1. Crystallographic data and parameters

Compound	(5)	(6)	(7)
Formula	C ₁₄ H ₃₀ CoCuN ₂ O ₁₄	C ₁₄ H ₃₆ N ₂ O ₁₇ Zn ₂	C ₁₄ H ₃₆ CoN ₂ O ₁₇ Zn
<i>M</i>	572.9	635.2	628.7
Space group	<i>Pbc</i> 2 ₁	<i>P</i> 2 ₁ / <i>n</i>	<i>P</i> 2 ₁ / <i>n</i>
Systematic absences	0 <i>kl</i> (<i>k</i> ≠ 2 <i>n</i>) 00 <i>l</i> (<i>l</i> ≠ 2 <i>n</i>) 0 <i>kl</i> (<i>l</i> ≠ 2 <i>n</i>) <i>h</i> 0 <i>l</i> (<i>l</i> ≠ 2 <i>n</i>)	<i>h</i> 0 <i>l</i> (<i>h</i> + <i>l</i> ≠ 2 <i>n</i>) 0 <i>kl</i> (<i>k</i> ≠ 2 <i>n</i>)	<i>h</i> 0 <i>l</i> (<i>h</i> + <i>l</i> ≠ 2 <i>n</i>) 0 <i>kl</i> (<i>k</i> ≠ 2 <i>n</i>)
<i>a</i> /Å	10.878(5)	9.702(2)	9.731(9)
<i>b</i> /Å	11.167(5)	11.757(2)	11.783(2)
<i>c</i> /Å	17.446(14)	20.980(5)	21.031(9)
β/°		95.61(2)	95.40(6)
<i>U</i> /Å ³	2 119(1)	2 352(1)	2 401(1)
<i>Z</i>	4	4	4
<i>D_c</i> /g cm ⁻³	1.80	1.77	1.74
<i>F</i> (000)	1 184	1 304	1 308
μ(Mo- <i>K</i> _α)/cm ⁻¹	18.6	21.5	17.0
Data collection instrument	Enraf-Nonius CAD-4	Enraf-Nonius CAD-4	Enraf-Nonius CAD-4
Radiation (graphite monochromated, λ = 0.70926 Å)	Mo- <i>K</i> _α	Mo- <i>K</i> _α	Mo- <i>K</i> _α
Scan mode	ω-2θ	ω-2θ	ω-2θ
2θ Range/°	2 < 2θ < 47° (<i>h</i> , ± <i>k</i> , <i>l</i>)	2 < 2θ < 50° (<i>h</i> , <i>k</i> , ± <i>l</i>)	2 < 2θ < 50° (± <i>h</i> , <i>k</i> , <i>l</i>)
Standard reflections	[113], [112]	[131], [545], [165] [120]	[128], [2410], [259]
Number of unique data, total with <i>l</i> > <i>n</i> σ(<i>l</i>)	1 642, 845 (<i>n</i> = 2.5)	4 183, 2 536 (<i>n</i> = 3)	4 252, 3 293 (<i>n</i> = 2.5)
Number of parameters refined	343	365	423
<i>R</i> ^{<i>a</i>}	0.056	0.098	0.041
<i>R</i> ^{<i>b</i>}	0.056	0.063	0.039
<i>w</i>	1	171.8223/ [σ ² (<i>F</i> _o) + 0.000 01 <i>F</i> _o ²]	28.9211/ [σ ² (<i>F</i> _o) + 0.000 012 <i>F</i> _o ²]
Largest shift/e.s.d. in final cycle	0.288	0.012	0.302
Largest peak/e Å ⁻³	0.5	1.0	0.8

$${}^a R = \Sigma(|F_o| - |F_c|)/\Sigma|F_o|, {}^b R' = [\Sigma w(|F_o| - |F_c|)^2/\Sigma w|F_o|^2]^{1/2}.$$

diffraction patterns were obtained by means of a Siemens Kristalloflex D500 diffractometer using Cu-*K*_α radiation. Compounds (1)–(5) are isostructural, having the same structure as [Zn(OH₂)₅][Cu(cdta)]·H₂O previously reported.¹⁰ Indexation and least-squares refinement of the patterns in the orthorhombic space group *Pbc*2₁, gave the following cell parameters for (1)–(4): (1), *a* = 10.88(2), *b* = 11.12(2), *c* = 17.44(1) Å; (2), *a* = 10.884(8), *b* = 11.165(8), *c* = 17.44(1) Å; (3), *a* = 10.881(6), *b* = 11.12(1), *c* = 17.41(2) Å; (4), *a* = 10.981(4), *b* = 11.114(8), *c* = 17.350(6) Å. Compounds (6)–(9) belong to the structural type D, and the cell parameters obtained for (8) and (9) by the same method using the monoclinic space group *P*2₁/*n* are: (8), *a* = 9.69(1), *b* = 11.78(1), *c* = 21.01(3) Å, β = 95.67(8)°; (9), *a* = 9.700(7), *b* = 12.191(7), *c* = 21.08(2) Å, β = 95.11(8)°.

Crystal Structure Determination of [Co(OH₂)₅][Cu(cdta)]·H₂O (5), [Zn(OH₂)₄][Zn(cdta)(OH₂)]·4H₂O (6), and [Zn_{0.7}Co_{0.3}(OH₂)₄][Zn_{0.3}Co_{0.7}Co(cdta)(OH₂)]·4H₂O (7).—The essential crystal characteristics and other data in the structure determinations are given in Table 1. The cell dimensions were derived from least-squares refinement of well centred reflections [number of reflections: 19 for (5), 6 < 2θ < 25°; 25 for (6) and (7), 14 < 2θ < 25°]. The structure of (6) was solved using direct methods (MULTAN 11/82¹³) to locate the two zinc atoms and successive Fourier synthesis to determine the positions of the

remaining non-hydrogen atoms. Compounds (5) and (7) were treated by using the final atomic co-ordinates of [Zn(OH₂)₅][Cu(cdta)]·H₂O¹⁰ and (6) respectively as starting data. Refinement of the structures was carried out with the SHELX 76¹⁴ system by weighted anisotropic full-matrix least squares. In each case the hydrogen atoms were either located by Fourier difference syntheses or placed in calculated positions and included in the final refinement with common isotropic thermal parameters [*U* = 0.050 for (5), 0.0514 for (6), and 0.0695 Å² for (7)]. In compounds (5) and (6) the hydrogen atoms of the water molecules were omitted from the model. In the case of complex (7), we have recently reported⁸ from visible spectra data the existence of an occupational disorder of the two metal atoms in the two co-ordination sites ('chelated' and 'hydrated') present in the molecule. In this way, this compound must be formulated as [Zn_{1-ε}Co_ε(OH₂)₄][Zn_εCo_{1-ε}(cdta)(OH₂)]·4H₂O, where ε indicates the occupation order degree and its predicted value from solution thermodynamic data [*i.e.* stability constants of [Zn(cdta)]²⁻ and [Co(cdta)]²⁻] is 0.41. Accordingly, in the refinement of this structure a fixed occupancy factor of 0.5 was initially assumed for each metal atom in each co-ordination position. After refinement to a *R* value of 0.042, and in order to determine the ε value, a set of subsequent independent refinements of the structure was carried out for 11 fixed ε values in the range 0.0–1.0. In each cycle, only the co-ordinates and

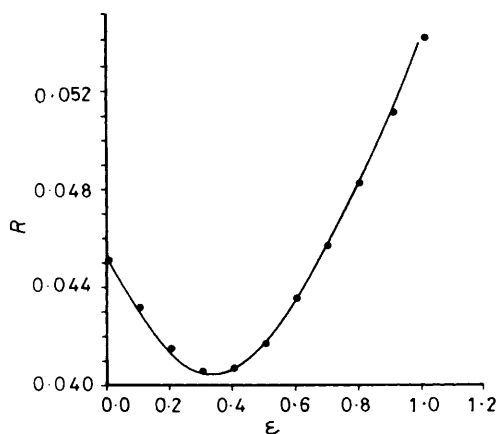


Figure 1. R factor [$R = \Sigma(|F_o| - |F_c|)/\Sigma|F_o|$] versus occupation order degree (ϵ) in the structure refinement of $[\text{Zn}_{1-\epsilon}\text{Co}_\epsilon(\text{OH}_2)_4]\text{[Zn}_\epsilon\text{Co}_{1-\epsilon}(\text{cdta})(\text{OH}_2)] \cdot 4\text{H}_2\text{O}$ (7)

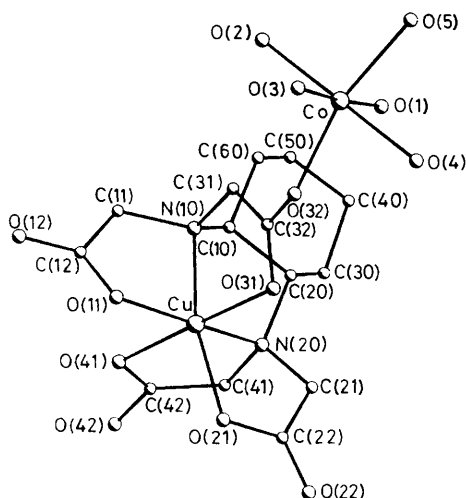


Figure 2. Perspective view and atomic numbering of $[\text{Co}(\text{OH}_2)_5]\text{[Cu}(\text{cdta})] \cdot \text{H}_2\text{O}$ (5)

anisotropic thermal parameters of the metal atoms were considered as variable parameters. The resulting values of R vs. ϵ are plotted in Figure 1. They were fitted to a polynomial function and a ϵ value of 0.34 was obtained for the minimum, which is close to the predicted thermodynamic value. Consequently, the formula $[\text{Zn}_{0.7}\text{Co}_{0.3}(\text{OH}_2)_4][\text{Zn}_{0.3}\text{Co}_{0.7}(\text{cdta})(\text{OH}_2)] \cdot 4\text{H}_2\text{O}$ was considered thereafter. Atomic scattering factors and anomalous terms for the metal atoms were chosen from International Tables.¹⁵ The geometrical calculations were carried out with XANADU¹⁶ and DISTAN¹⁷ and molecular illustrations were drawn with PLUTO.¹⁸ The final atomic coordinates are given in Tables 2 and 3, and the selected bond distances and angles in Tables 4 and 5. Figures 2 and 3 show perspective views of the molecules and Figure 4 a stereoscopic view of the unit cell for (6) and (7).

Additional material available from the Cambridge Crystallographic Data Centre comprises H-atom co-ordinates, thermal parameters and remaining bond distances and angles.

Magnetic Measurements.—Magnetic susceptibilities were measured in the range 4–100 K with a pendulum-type apparatus equipped with a helium cryostat. Measurements from 4.2 to 1 K were made in a glass cryostat with pumped liquid helium. The uncertainty in the data is <0.1 K for temperature

Table 2. Fractional atomic co-ordinates ($\times 10^3$, Cu and Co $\times 10^4$) for (5) with estimated standard deviations (e.s.d.s) in parentheses

Atom	X/a	Y/b	Z/c
Cu	-1 686(4)	572(3)	204
Co	-2 241(5)	-1 869(4)	-2 827(3)
N(10)	-113(3)	127(2)	-79(1)
N(20)	-315(3)	176(2)	20(2)
O(1)	-325(2)	-26(2)	-289(1)
O(2)	-67(3)	-89(2)	-313(1)
O(3)	-118(3)	-343(2)	-284(1)
O(4)	-376(3)	-299(2)	-253(1)
O(5)	-284(3)	-219(2)	-398(1)
O(6)	371(3)	165(2)	-95(1)
O(11)	-3(2)	-18(2)	21(2)
O(12)	194(3)	49(2)	-2(1)
O(21)	-268(3)	-13(2)	109(1)
O(22)	-459(3)	-28(2)	151(1)
O(31)	-253(3)	-82(2)	-53(1)
O(32)	-212(3)	-164(2)	-165(1)
O(41)	-88(2)	205(2)	96(1)
O(42)	-148(3)	358(2)	168(1)
C(10)	-191(3)	239(3)	-91(2)
C(11)	26(3)	146(3)	-66(2)
C(12)	77(4)	54(3)	-10(1)
C(20)	-324(4)	220(3)	-65(2)
C(21)	-415(3)	100(3)	42(2)
C(22)	-384(3)	13(3)	104(2)
C(30)	-398(3)	335(3)	-77(2)
C(31)	-137(4)	35(3)	-140(2)
C(32)	-201(4)	-76(3)	-118(2)
C(40)	-397(5)	369(4)	-163(2)
C(41)	-294(4)	276(3)	80(2)
C(42)	-171(3)	279(3)	114(2)
C(50)	-273(4)	398(3)	-185(2)
C(60)	-201(5)	291(3)	-174(2)

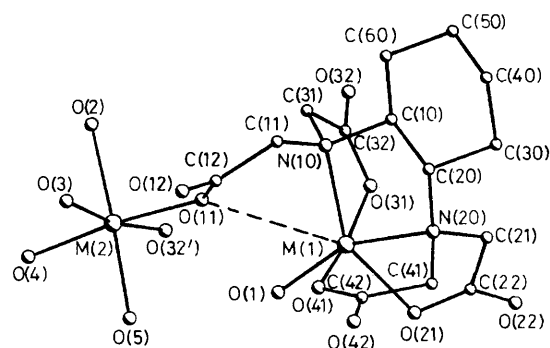


Figure 3. Perspective view and atomic numbering of $[\text{M}(2)(\text{OH}_2)_4]\text{[M}(1)(\text{cdta})(\text{OH}_2)] \cdot 4\text{H}_2\text{O}$ [$\text{M}(1)$, $\text{M}(2) = \text{Zn}$ in (6), Zn and Co in (7)]. $\text{O}(32')$ is obtained from $\text{O}(32)$ through the symmetry operation $1 - x, 1 - y, -z$

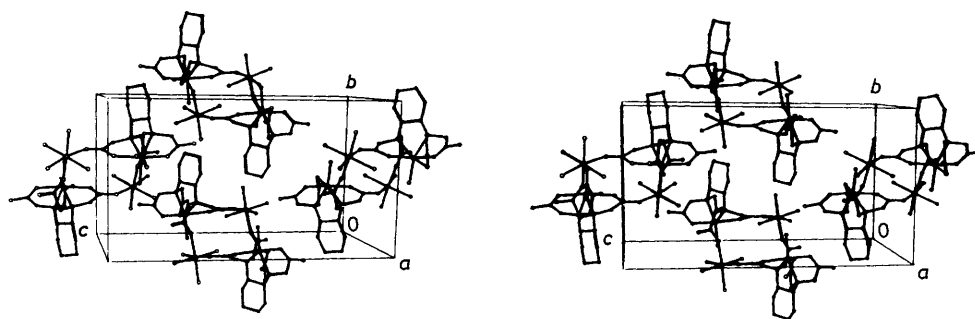
and $<2 \times 10^{-5}$ e.m.u. mol^{-1} (e.m.u. = S.I. $\times 10^6/4\pi$) for susceptibility.

Results and Discussion

Crystal Structure of $[\text{Co}(\text{OH}_2)_5][\text{Cu}(\text{cdta})] \cdot \text{H}_2\text{O}$ (5).—The structure consists of dimeric entities, constructed from cationic $[\text{Co}(\text{OH}_2)_5]^{2+}$ and anionic $[\text{Cu}(\text{cdta})]^{2-}$ molecules which are linked through a bridging carboxylate group from the cdta ligand. The two metal atoms are six-co-ordinated. In the anionic ('chelated') position, the copper atom is bound to two nitrogen atoms and four oxygen atoms from cdta, that acts as a

Table 3. Fractional atomic co-ordinates for complexes (6) ($\times 10^4$) and (7) ($\times 10^4$, Zn and Co $\times 10^5$) with e.s.d.s in parentheses

Atom	(6)			(7)		
	X/a	Y/b	Z/c	X/a	Y/b	Z/c
M(1)	3 563(2)	3 879(1)	1 356(1)	35 630(6)	38 720(5)	13 582(3)
M(2)	7 584(2)	6 299(1)	1 299(1)	75 897(6)	62 796(5)	12 963(3)
N(10)	5 187(10)	2 733(8)	1 066(5)	5 176(4)	2 726(3)	1 065(2)
N(20)	2 670(11)	2 302(8)	1 661(5)	2 690(4)	2 292(4)	1 663(2)
O(1)	3 807(9)	5 584(7)	1 283(5)	3 800(4)	5 582(3)	1 284(2)
O(2)	8 838(9)	5 626(7)	598(4)	8 851(4)	5 618(3)	592(2)
O(3)	9 331(9)	5 722(7)	1 959(4)	9 324(4)	5 722(4)	1 960(2)
O(4)	8 346(9)	7 930(7)	1 244(4)	8 328(4)	7 900(3)	1 245(2)
O(5)	6 507(9)	6 919(7)	2 038(4)	6 509(5)	6 899(3)	2 029(2)
O(6)	3 756(11)	3 448(7)	5 149(5)	3 746(5)	3 466(4)	5 152(2)
O(7)	3 442(9)	1 754(7)	4 217(5)	3 426(5)	1 756(4)	4 235(2)
O(8)	6 441(10)	4 174(8)	4 816(4)	6 482(5)	4 164(4)	4 818(2)
O(9)	5 989(11)	5 421(8)	2 984(5)	5 996(5)	5 396(3)	2 988(2)
O(11)	6 627(9)	4 743(7)	1 398(4)	6 625(4)	4 730(3)	1 399(2)
O(12)	7 888(9)	3 901(7)	2 220(4)	7 880(4)	3 879(3)	2 218(2)
O(21)	1 366(9)	4 261(6)	1 363(4)	1 376(4)	4 243(3)	1 351(2)
O(22)	- 544(9)	3 425(7)	901(5)	- 532(4)	3 409(3)	902(2)
O(31)	3 113(9)	3 730(8)	331(4)	3 103(4)	3 754(3)	331(2)
O(32)	4 070(9)	3 388(7)	- 583(4)	4 045(4)	3 395(3)	- 574(2)
O(41)	4 252(9)	3 872(7)	2 321(4)	4 249(4)	3 864(3)	2 324(2)
O(42)	4 041(10)	3 009(8)	3 246(4)	4 018(4)	3 020(4)	3 244(2)
C(10)	4 521(14)	1 555(10)	1 030(7)	4 515(6)	1 554(4)	1 015(3)
C(11)	6 476(14)	2 726(11)	1 519(7)	6 456(6)	2 716(4)	1 516(3)
C(12)	7 029(12)	3 887(11)	1 724(5)	7 012(5)	3 871(4)	1 729(2)
C(20)	3 666(14)	1 361(10)	1 585(6)	3 681(5)	1 343(4)	1 587(3)
C(21)	1 322(14)	2 220(10)	1 262(6)	1 351(6)	2 208(5)	1 267(3)
C(22)	663(13)	3 410(10)	1 175(6)	690(6)	3 375(5)	1 174(3)
C(30)	2 946(17)	187(12)	1 548(8)	3 008(6)	165(5)	1 553(3)
C(31)	5 417(14)	3 078(11)	414(7)	5 443(6)	3 085(5)	409(3)
C(32)	4 094(13)	3 417(9)	24(6)	4 097(5)	3 434(4)	27(3)
C(40)	4 098(17)	9 224(10)	1 474(9)	4 060(7)	- 773(5)	1 480(3)
C(41)	2 518(14)	2 461(11)	2 343(6)	2 496(6)	2 447(5)	2 343(3)
C(42)	3 725(14)	3 159(10)	2 656(6)	3 693(6)	3 151(5)	2 663(3)
C(50)	4 832(17)	- 548(11)	904(8)	4 825(7)	- 561(5)	896(3)
C(60)	5 556(15)	601(11)	952(7)	5 563(6)	589(5)	962(3)

**Figure 4.** Stereoscopic view of the unit cell showing the tetranuclear entities in $[M(2)(OH_2)_4][M(1)(cdta)(OH_2)] \cdot 4H_2O$ [$M(1), M(2) = Zn$ in (6), Zn and Co in (7)]

sexidentate ligand. The co-ordination polyhedron of this metal atom can be described as a tetragonally-elongated octahedron. As occurs in the similar complexes $[Cu(OH_2)_4][Cu(cdta)]^9$ and $[Zn(OH_2)_5][Cu(cdta)] \cdot H_2O$,¹⁰ the basal plane comprises the two nitrogen atoms and two oxygen atoms [O(11), O(21)] from type G carboxylates. The axial positions are occupied by two oxygen atoms [O(31), O(41)] belonging to type R carboxylates, which are placed at significantly longer distances from the copper atom than the equatorial ones [Cu-N (av.) 2.03(4), Cu-O_G (av.) 2.01(3), Cu-O_R (av.) 2.25(3) Å]. (The subscripts R and G indicate the chelate rings whose mean plane is nearly perpendicular or parallel, respectively, to the

N-M-N' plane, as established by Weakliem and Hoard.¹⁹) In this way, the co-ordination of the copper atom is 4 + 2,²⁰ with a tetragonality T (defined as the mean in-plane Cu-O,N bond length divided by the mean out-of-plane bond length, R_S/R_L) of 0.89.²¹ This value is similar to that found in the isostructural $[Zn(OH_2)_5][Cu(cdta)] \cdot H_2O$, but is greater than that shown in the chelated site by the copper homometallic derivative $[Cu(OH_2)_4][Cu(cdta)]$ ($T = 0.83$), which implies a greater octahedral distortion in the latter resulting from a co-operative Jahn-Teller effect.⁹

Interatomic distances and angles within the cdta ligand are in the usual range. This shows the $E,G/R$ configuration,²² as

Table 4. Selected bond distances (Å) and angles (°) in (5) with e.s.d.s in parentheses

N(10)-Cu	1.99(2)	O(5)-Co	2.15(2)
N(20)-Cu	2.07(3)	O(32)-Co	2.07(2)
O(11)-Cu	1.99(2)	C(12)-O(11)	1.30(4)
O(21)-Cu	2.03(2)	C(12)-O(12)	1.28(4)
O(31)-Cu	2.21(2)	C(22)-O(21)	1.30(4)
O(41)-Cu	2.29(2)	C(22)-O(22)	1.23(4)
O(1)-Co	2.11(2)	C(32)-O(31)	1.28(4)
O(2)-Co	2.09(3)	C(32)-O(32)	1.29(4)
O(3)-Co	2.09(2)	C(42)-O(41)	1.26(4)
O(4)-Co	2.13(3)	C(42)-O(42)	1.32(4)
N(20)-Cu-N(10)	89(1)	O(4)-Co-O(3)	87(1)
O(11)-Cu-N(10)	84(1)	O(5)-Co-O(1)	86.5(9)
O(11)-Cu-N(20)	164.9(9)	O(5)-Co-O(2)	95.6(9)
O(21)-Cu-N(10)	165(1)	O(5)-Co-O(3)	91(1)
O(21)-Cu-N(20)	81(1)	O(5)-Co-O(4)	83.8(9)
O(21)-Cu-O(11)	108(1)	O(32)-Co-O(1)	88.6(9)
O(31)-Cu-N(10)	84.3(9)	O(32)-Co-O(2)	98(1)
O(31)-Cu-N(20)	97(1)	O(32)-Co-O(3)	95(1)
O(31)-Cu-O(11)	95(1)	O(32)-Co-O(4)	83(1)
O(31)-Cu-O(21)	86.8(8)	O(32)-Co-O(5)	166(1)
O(41)-Cu-N(10)	95.9(9)	C(12)-O(11)-Cu	110(2)
O(41)-Cu-N(20)	80.4(9)	C(22)-O(21)-Cu	113(2)
O(41)-Cu-O(11)	87.2(9)	C(32)-O(31)-Cu	107(2)
O(41)-Cu-O(21)	92.6(9)	C(32)-O(32)-Co	137(2)
O(41)-Cu-O(31)	178(1)	C(42)-O(41)-Cu	110(2)
O(2)-Co-O(1)	88.2(9)	O(12)-C(12)-O(11)	127(3)
O(3)-Co-O(1)	176.0(9)	O(22)-C(22)-O(21)	122(3)
O(3)-Co-O(2)	89(1)	O(32)-C(32)-O(31)	119(3)
O(4)-Co-O(1)	96.2(9)	O(42)-C(42)-O(41)	119(3)
O(4)-Co-O(2)	175.5(9)		

in the previously reported structures of bimetallic cdta complexes,⁹⁻¹¹ and the cyclohexane ring is in the chair form. The monodentate carboxylate groups are all asymmetric, the C-O bond distances satisfying the expected relation $d_{C-O(1)} > d_{C-O(2)}$ (owing to the polarization of the charge density towards the metal-bonded oxygen atoms) for COO_G groups and the inverse relation $d_{C-O(1)} < d_{C-O(2)}$ for the COO_R . This inversion of the asymmetry in COO_R groups is general in the bimetallic complexes of edta-like ligands having a copper atom occupying the 'chelated' position (see ref. 9), and reflects the semi-co-ordinated character of the oxygen atoms belonging to these groups in this co-ordination site. The bridging COO_R group is nearly symmetrical, and its structural function is intermediate between $a-2-s$ and $a-2-a$ (nearer to $a-2-a$), after the terminology established by Porai-Koshits.^{23,*}

The co-ordination polyhedron of the Co atom in the cationic ('hydrated') site is a slightly distorted octahedron, with normal Co-O distances for this type of environment. The intermolecular packing is achieved by hydrogen bonding between the six water molecules and the oxygen atoms from carboxylate groups and other symmetry-related water molecules.

Crystal Structures of $[Zn(OH_2)_4][Zn(cdta)(OH_2)] \cdot 4H_2O$ (6) and $[Zn_{0.7}Co_{0.3}(OH_2)_4][Zn_{0.3}Co_{0.7}(cdta)(OH_2)] \cdot 4H_2O$ (7).—As in the structural types A, B, C, and E of bimetallic compounds of cdta, the two metal atoms in (6) and (7) occupy two different co-ordination positions in the lattice. The metal atom M(1) is bound in the chelated position to two nitrogen atoms, three oxygen atoms from the cdta, one water molecule, and further semi-co-ordinated to a fourth oxygen atom of the

ligand. In the hydrated position the second metal atom M(2) is co-ordinated to four water molecules and two oxygen atoms belonging to carboxylate groups from two adjacent $[M(1)-(cdta)(OH_2)]^{2-}$ entities. The above species $[M(1)-(cdta)(OH_2)]^{2-}$ and $[M(2)(OH_2)_4]^{2+}$ sharing two oxygen atoms [O(11), O(32)] of different carboxylate groups alternate in order to form tetranuclear units having a crystallographic centre in the plane formed by the four metal atoms (see Figures 3 and 4).

The co-ordination of the M(1) metal atom can be considered as $6+1$. The two nitrogen atoms, three oxygen atoms from the ligand {belonging to two carboxylate groups of R type [O(31), O(41)] and one of G type [O(21)]}, and the water molecule O(1) are placed at normal bond distances from this metal, forming a *cis*-distorted octahedron around it. The high angular deviations from idealized octahedral values of this polyhedron, together with the X-M(1)-O(11) [X = N(10), N(20), O(21), O(31), O(41), or O(1)] observed angles provide evidence for the incipient formation of a seventh bond to M(1) from the oxygen atom O(11) belonging to the second type G carboxylate M(1)-O(11) = 3.135(8) in (6) and 3.139(7) Å in (7)]. This configuration is very similar to that showed by the complex ion $[Co(edta)(OH_2)]^{2-}$ in the compound $Ca[Co(edta)(OH_2)] \cdot 4H_2O$ (Co-N = 2.195, 2.227 Å; Co-O_R = 2.133, 2.074 Å; Co-O_G = 2.731, 2.205 Å; Co-O_w = 2.062 Å).²⁴

The co-ordination polyhedra of seven-co-ordinate edta-like complexes are usually described as a pentagonal bipyramid (pbp, D_{5h} symmetry) or a single-cap trigonal prism (stp, C_{2v} symmetry), associated to the $E,G/R$ and $E,R/G$ ²² ligand configurations respectively.

In (6) and (7), if we consider the pbp geometry, the equatorial plane is defined by the two nitrogen atoms, the two G oxygen atoms [O(11), O(21)], and the water molecule [O(1)], the axial positions being occupied by the two R oxygen atoms. For the stp geometry, the capped face is formed by the four oxygen atoms from the edta, and the water molecule occupies the capping position. Comparison of the observed angles around the metal atoms with the ideal values established for both stereochemistries²⁵ clearly indicates a greater parallelism with the stp parameters. This is also reflected when comparing the averaged angles (assuming a two-fold axis that passes through the water molecule, the metal atom, and the centre of the cyclohexane ring) of these complexes with those corresponding to the complex ions $[Fe(edta)(OH_2)]^-$ (pbp geometry),²⁶ $[Co(edta)(OH_2)]^{2-}$ and $[Fe(cdta)(OH_2)]^-$ (stp geometry)^{24,27} (see Table 6). The ligand configuration is $E,R/G$ in both (6) and (7), in agreement with the observed stp geometry and contrary to the other structural types of bimetallic compounds of cdta. The cyclohexane ring is in the chair form. The unidentate carboxylate groups are both asymmetric in (6) and (7), and the observed C-O bond distances are related to the relative strength of the metal-oxygen and hydrogen bonds involved. The bridging COO_R group is nearly symmetrical and its structural function is $a-2-s$ [torsion angles: M(1)-O(31)-C(32)-O(32), -172.6 for (6) and -174.8° for (7); M(2)-O(32)-C(32)-O(31), 5.5 for (6) and 3.7° for (7)]. The iminoacetate bridge M(1)-N(10)-C(11)-C(12)-O(11)-M(2) is formed as a result of the quasi-opening of a G ring from the sixidentate ligand. This is consistent with the fact that in edta-like complexes, G rings but not R ones open normally on protonation or upon co-ordination of the metal atom to a monodentate ligand owing to their greater angular strain.^{22,28}

Bond distances around the hydrated metal atom M(2) are divided into two groups: M(2)-O(2), O(3), O(32'); $\bar{d} = 2.152(15)$ Å for (6) and 2.158(7) Å for (7); M(2)-O(4), O(5), O(11); $\bar{d} = 2.073(14)$ for (6) and 2.066(8) Å for (7). The resulting co-ordination polyhedron is a distorted octahedron with an idealized point symmetry C_{2v} . There are three hydrogen bonds

* Principal number = total co-ordination capacity of carboxylate, $a = anti$, and $s = syn$.

Table 5. Selected bond distances (Å) and angles (°) in (6) and (7) with e.s.d.s in parentheses; O(32') is related to the atom O(32) listed in Table 3 through the symmetry operation $1 - x, 1 - y, -z$

	(6)	(7)		(6)	(7)
N(10)-M(1)	2.204(11)	2.202(4)	O(11)-M(2)	2.070(8)	2.074(4)
N(20)-M(1)	2.169(10)	2.168(4)	O(32')-M(2)	2.120(8)	2.128(4)
O(1)-M(1)	2.026(8)	2.036(4)	C(12)-O(11)	1.26(1)	1.265(6)
O(21)-M(1)	2.179(9)	2.171(4)	C(12)-O(12)	1.27(1)	1.268(6)
O(31)-M(1)	2.158(8)	2.169(4)	C(22)-O(21)	1.25(1)	1.257(6)
O(41)-M(1)	2.069(8)	2.077(3)	C(22)-O(22)	1.25(1)	1.271(7)
O(2)-M(2)	2.148(10)	2.157(4)	C(32)-O(31)	1.26(2)	1.266(7)
O(3)-M(2)	2.189(8)	2.188(4)	C(32)-O(32)	1.27(2)	1.262(6)
O(4)-M(2)	2.063(8)	2.046(4)	C(42)-O(41)	1.24(2)	1.257(7)
O(5)-M(2)	2.085(9)	2.079(5)	C(42)-O(42)	1.26(2)	1.244(6)
	(6)	(7)		(6)	(7)
N(20)-M(1)-N(10)	82.9(4)	82.3(2)	O(11)-M(2)-O(4)	173.5(4)	172.6(2)
O(1)-M(1)-N(10)	119.5(4)	119.8(2)	O(11)-M(2)-O(5)	88.4(4)	88.1(2)
O(1)-M(1)-N(20)	157.1(4)	157.4(2)	O(2)-M(2)-O(32')	91.1(4)	90.6(2)
O(21)-M(1)-N(10)	148.6(3)	147.7(1)	O(3)-M(2)-O(32')	171.0(4)	171.7(2)
O(21)-M(1)-N(20)	75.8(3)	76.3(1)	O(4)-M(2)-O(32')	92.9(4)	92.1(2)
O(21)-M(1)-O(1)	85.3(3)	85.3(1)	O(5)-M(2)-O(32')	93.8(4)	94.0(2)
O(31)-M(1)-N(10)	75.9(3)	76.6(1)	O(11)-M(2)-O(32')	84.8(4)	85.3(2)
O(31)-M(1)-N(20)	100.2(4)	100.9(2)	C(12)-O(11)-M(2)	130.0(7)	130.3(3)
O(31)-M(1)-O(1)	91.1(4)	90.1(2)	C(22)-O(21)-M(1)	109.6(7)	109.3(3)
O(31)-M(1)-O(21)	85.5(3)	84.0(1)	C(32)-O(31)-M(1)	116.5(7)	115.2(3)
O(41)-M(1)-N(10)	95.5(4)	95.7(1)	C(42)-O(41)-M(1)	116.6(8)	116.2(3)
O(41)-M(1)-N(20)	79.0(4)	78.8(2)	O(12)-C(12)-O(11)	126(1)	125.5(5)
O(41)-M(1)-O(1)	92.8(4)	92.9(2)	C(11)-C(12)-O(11)	116(1)	116.1(4)
O(41)-M(1)-O(21)	102.5(4)	103.5(2)	C(11)-C(12)-O(11)	119(1)	118.4(4)
O(41)-M(1)-O(31)	171.4(3)	172.2(1)	O(22)-C(22)-O(21)	126(1)	123.7(5)
O(3)-M(2)-O(2)	82.2(3)	82.8(2)	C(21)-C(22)-O(21)	119(1)	119.4(5)
O(4)-M(2)-O(2)	94.3(4)	94.4(2)	C(21)-C(22)-O(22)	115(1)	116.9(5)
O(4)-M(2)-O(3)	93.6(3)	93.5(2)	O(32)-C(32)-O(31)	126(1)	123.8(5)
O(5)-M(2)-O(2)	175.1(3)	175.4(2)	C(31)-C(32)-O(31)	116(1)	118.3(4)
O(5)-M(2)-O(3)	92.9(4)	92.6(2)	C(31)-C(32)-O(32)	118(1)	117.9(5)
O(5)-M(2)-O(4)	85.7(4)	85.2(2)	O(42)-C(42)-O(41)	126(1)	123.8(5)
O(11)-M(2)-O(2)	91.9(4)	92.6(1)	C(41)-C(42)-O(41)	118(1)	117.6(5)
O(11)-M(2)-O(3)	89.4(3)	89.9(1)	C(41)-C(42)-O(42)	117(1)	118.5(5)

Table 6. Averaged angles^a for the complex anions [Zn(cdda)(OH₂)²⁻, [M(1)(cdda)(OH₂)²⁻, [Fe(edta)(OH₂)⁻, [Co(edta)(OH₂)²⁻, and [Fe(cdda)(OH₂)⁻ in the respective complexes [Zn(OH₂)₄][Zn(cdda)(OH₂)⁻·4H₂O, [Zn_{0.7}Co_{0.3}(OH₂)₄][Zn_{0.3}Co_{0.7}(cdda)(OH₂)⁻·4H₂O, Li[Fe(edta)(OH₂)⁻·2H₂O,²⁶ Ca[Co(edta)(OH₂)⁻·4H₂O,²⁴ and Ca[Fe(cdda)(OH₂)⁻·8H₂O²⁷

Angle	[Zn(cdda)- OH ₂] ²⁻	[M(1)(cdda)- (OH ₂) ²⁻	[Fe(edta)- (OH ₂) ⁻	[Co(edta)- (OH ₂) ²⁻	[Fe(cdda)- (OH ₂) ⁻
O _R -M-N ^b	77.5	77.7	78.9	77.0	75.7
O _R -M-N ^c	97.9	98.3	89.7	102.6	100.0
O _R -M-O _G ^d	100.7	101.2	93.4	102.8	99.5
O _R -M-O _G ^e	80.8	80.0	90.9	77.2	82.1
O _R -M-O _w	92.0	91.5	97.1	89.8	92.9
O _G -M-N ^f	68.1	68.4	71.3	69.2	71.8
O _G -M-O _w	74.7	74.9	72.5	77.6	74.6
N-M-N	82.9	82.3	73.7	79.4	76.5
O _R -M-O _R	171.4	172.2	165.6	175.3	173.8
O _G -M-O _G	149.2	149.6	144.8	155.1	148.9

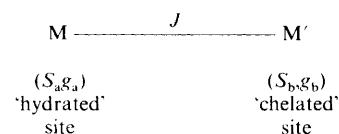
^a In agreement with a two-fold axis. ^b O_R and N in the same ring. ^c O_R and N in different rings sharing M. ^d O_R and O_G in rings sharing a M-N bond. ^e O_R and O_G in rings sharing M. ^f O_G and N in the same ring.

within each tetranuclear entity, between the water molecules [O(1), O(2), and O(3)] and the oxygen atoms from carboxylate groups [O(32), O(31), and O(12)] respectively. Different tetranuclear entities interact through hydrogen bonds involving crystallization or co-ordination water molecules and oxygen atoms from carboxylate groups. The strongest hydrogen bonds

are formed by the unco-ordinated oxygen atoms O(*i*) (*i* = 1, 2, or 4).

Magnetic Properties.—The magnetic behaviour of compounds (1), (2), (3), (9), (4), (5), and (8) are shown in Figure 5. Compound (1) displays a maximum in susceptibility centred at $T \approx 10$ K [Figure 5(a)], followed by Curie-Weiss law at higher temperatures. Such features agree with the presence of an intramolecular antiferromagnetic coupling between the Ni^{II} ions. The remaining compounds exhibit a continuous increase in susceptibility upon cooling. The plot in these systems of $\chi_m T$ (proportional to $\mu_{\text{eff.}}^2$) vs. T shows a decrease as the temperature is lowered, which also indicates the existence of weak antiferromagnetic interactions between the metal ions.

Analysis of the Magnetic Data.—From the structural results all these compounds can be considered as dimers in which the metal atoms M and M', having different spins (*S*) and Landé factors (*g*), are coupled by an exchange J^* (see below). For



* In compounds belonging to structural type D, the iminoacetate bridges do not provide support for the propagation of magnetic interactions.

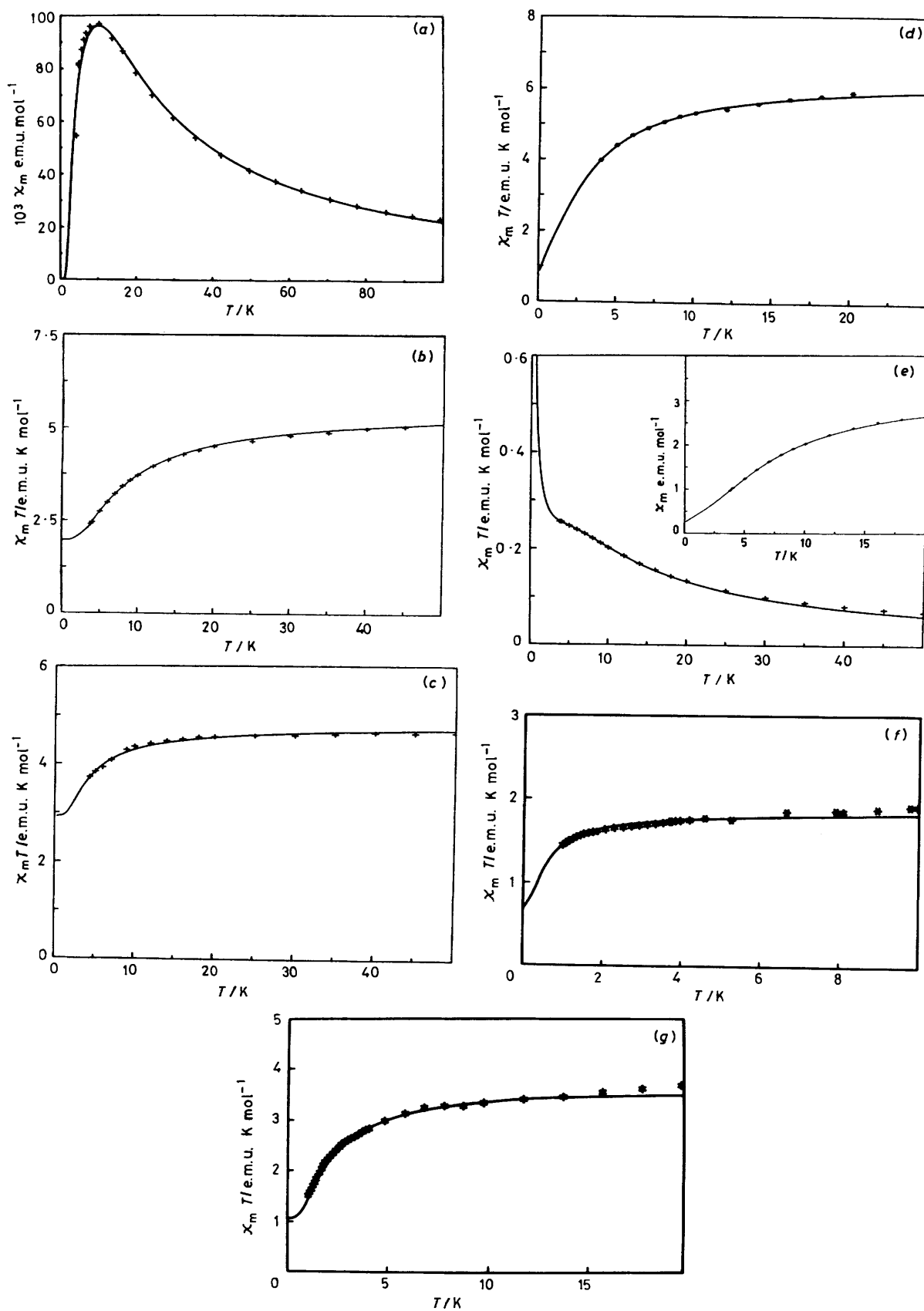


Figure 5. Magnetic behaviour of (a) $[\text{Ni}(\text{OH}_2)_5][\text{Ni}(\text{cdta})]\cdot\text{H}_2\text{O}$ (1), (b) $[\text{Mn}(\text{OH}_2)_5][\text{Ni}(\text{cdta})]\cdot\text{H}_2\text{O}$ (2), (c) $[\text{Mn}(\text{OH}_2)_5][\text{Cu}(\text{cdta})]\cdot\text{H}_2\text{O}$ (3), (d) $[\text{Mn}(\text{OH}_2)_4][\text{Co}(\text{cdta})(\text{OH}_2)]\cdot 4\text{H}_2\text{O}$ (9), (e) $[\text{Co}(\text{OH}_2)_5][\text{Ni}(\text{cdta})]\cdot\text{H}_2\text{O}$ (4), (f) $[\text{Co}(\text{OH}_2)_5][\text{Cu}(\text{cdta})]\cdot\text{H}_2\text{O}$ (5), and (g) $[\text{Co}(\text{OH}_2)_4][\text{Co}(\text{cdta})(\text{OH}_2)]\cdot 4\text{H}_2\text{O}$ (8)

such a magnetic system, the general expression of the spin Hamiltonian to be solved is shown by equation (1), where H is

$$\mathcal{H} = -[J_{\parallel}S_{az}S_{bz} + J_{\perp}(S_{ax}S_{bx} + S_{ay}S_{by})] - [g_{a\parallel}S_{az} + g_{b\parallel}S_{bz}] \beta H^z - [g_{a\perp}(S_{ax} + S_{ay}) + g_{b\perp}(S_{bx} + S_{by})] \beta H^x + D_a S_{az}^2 + D_b S_{bz}^2 \quad (1)$$

the applied magnetic field, β is the Bohr magneton, and D_i ($i = a$ or b) is the zero-field splitting parameter of the Ni^{II} ion. By putting either $J_{\perp} = 0$ or $J_{\parallel} = 0$ one obtains the Ising and XY models, respectively, whereas the case $J_{\perp} = J_{\parallel} = J$ corresponds to the isotropic Heisenberg model. As the spin Hamiltonian is written, D is positive when the splitting of the ${}^3A_{2g}$ Ni^{II} ground state gives rise to a singlet ($M_s = 0$), which is at lower energy than the doublet state ($M_s = \pm 1$). In general, the zero-field magnetic susceptibilities of these systems have to be obtained by a computational procedure that involves the diagonalization of a $(2S_a + 1)(2S_b + 1)$ energy matrix.²⁶

Complex (1). For this system, in which $S_a = S_b = 1$, magnetic data can be satisfactorily fitted from a Heisenberg model by considering an exchange coupling $J = -6.8 \text{ cm}^{-1}$ and a mean $g = 2.19$ [see Figure 5(a)]. It does not seem necessary to introduce further parameters into the fit. This fact might indicate that g -alternation and local anisotropy effects are too slight to be detected in the reported temperature range. Anyway, in the region of the maximum of χ_m both effects may compensate one another, since while the g -alternation leads to an increase in the height of the maximum, a decrease occurs if positive zero-field splittings are considered.

Complexes (2) and (3). According to the orbitally non-degenerate ground state of the involved ions, these compounds may be viewed as S_a-S_b dimers [with $S_a(\text{Mn}^{\text{II}}) = \frac{5}{2}$ and $S_b(\text{Ni}^{\text{II}} \text{ or } \text{Cu}^{\text{II}}) = 1$ or $\frac{1}{2}$], coupled by an isotropic exchange. A good agreement with experiment is obtained for the two complexes by assuming a Heisenberg model and keeping $g_a = 2$ constant in the fits [Figure 5(b) and (c)]. The resulting J and g_b values are: $J = -2.2 \text{ cm}^{-1}$, $g_b = 2.15$ [(2)] and $J = -2.1 \text{ cm}^{-1}$, $g_b = 2.13$ [(3)]. As in the case of (1) it does not seem necessary to take into account the influence of the Ni^{II} zero-field splitting on the susceptibility data of (2). The ground state of this system is expected to be very sensitive to the ratio $D/|J|$. So, whereas in the case $D \ll |J|$ a $S = \frac{3}{2}$ ground state can be expected to arise from an antiferromagnetic coupling between the two local spins, when $D \gg |J|$ the system is dominated by single-ion effects so that the low-temperature behaviour must approach that of a single Mn^{II} ion ($S = S_a = \frac{5}{2}$). Then, magnetic measurements at lower temperatures could allow some information about the D parameters to be obtained.

Complexes (9), (4), (5) and (8). In discussing the magnetic properties of these complexes we have to bear in mind that in distorted O_h symmetry the high-spin Co^{II} ion behaves at low temperatures as an anisotropic spin doublet. This results from the combination of crystal-field distortion and spin-orbit coupling, which split the ${}^4T_{1g}$ ground term into six Kramers doublets that are well separated in energy.^{29,30} The spin anisotropy of Co^{II} is reflected in the g components. Thus, g values obtained from e.s.r. experiments for Co^{II} in similar environments to those found in these compounds, i.e. in $[\text{Co}(\text{OH}_2)_4][\text{Co}(\text{edta}) \cdot 2\text{H}_2\text{O}]$, are $g_{\parallel a} = 5.9$, $g_{\perp a} = 3.9$, $g_{\parallel b} = 10.1$, and $g_{\perp b} = 1.3$.³¹ As a consequence of the strong anisotropy in the g components, a large anisotropy of the exchange interaction is expected since the Co^{II} ion establishes a preference for the moments to align parallel to the z axis. Then, the anisotropic Ising model should be closely approximated in the four systems under consideration.

The magnetic behaviour of (9) in the range 1–30 K is shown in Figure 5(d). By fixing $g_{\parallel a} = 2$ in the fitting procedure, a good

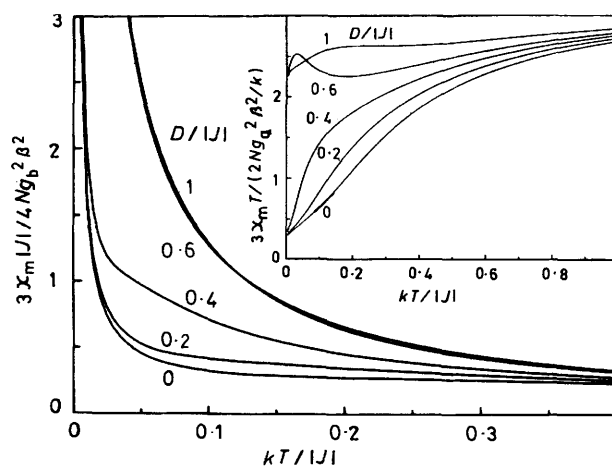


Figure 6. Influence of the zero-field splitting of Ni^{II} on the magnetic susceptibility of an antiferromagnetically coupled Ising dimer with $S_a = \frac{1}{2}$ and $S_b = 1$. Values of Landé components close to those found in the fit of the data of (4) have been considered ($g_{\parallel a} = 3.5$, $g_{\perp b} = 2$, $g_{\perp a}$)

agreement with experimental data is obtained by considering an $S_a = \frac{5}{2}$, $S_b = \frac{1}{2}$ Ising dimer for $J = -3.5 \text{ cm}^{-1}$, $g_{\parallel \text{Co}} = 5.13$, and $g_{\perp \text{Co}} = 4.2$.

Susceptibility data at $T < 20 \text{ K}$ for (4) fit to an Ising dimer with $S_a = \frac{1}{2}$, $S_b = 1$, and $J = -14.7 \text{ cm}^{-1}$ [Figure 5(e)]. Resulting Landé factors are $g_{\parallel \text{Co}} = 7.0$, $g_{\perp \text{Co}} = 3.3$, and $g_{\text{Ni}} = 2.10$. As in the case of (1), it does not seem necessary to introduce into the fit the zero-field splitting of Ni^{II} . In order to determine the influence of this parameter we have calculated the theoretical curves of susceptibility for several values of the $D/|J|$ ratio, keeping the Landé factors close to those found in (4) (Figure 6). From these curves we observe that an increase in the $D/|J|$ ratio leads to a large divergence of χ_m at low temperatures. The plot of $\chi_m T$ vs. T is here more informative since this is very sensitive to the net magnetic moment within the ground state of the dimer. Thus, $\chi_m T$ shows a continuous decrease with T when $D/|J|$ values are close to zero ($D/|J| < 0.5$), according to the weak resulting magnetic moment within the ground state (remember that in the Ising model, the exact cancellation of the two magnetic moments occurs when $g_{\parallel a}S_a = g_{\parallel b}S_b$).³² On the other hand $\chi_m T$ stays relatively constant for $D/|J| > 0.5$ according to the magnetic moment of the Co^{II} ion which dominates the low-temperature behaviour (Ni^{II} is in a non-magnetic ground state). In our case, the experimental behaviour is in agreement with $D/|J| < 0.5$ which supports a D value lower than ca. 7 cm^{-1} . In fact, for the 'chelated' Ni^{II} ion of the edta family, a value of D around 6 cm^{-1} has been calculated from specific heat measurements.³³

For a $S = \frac{1}{2}$ Ising dimer with different g factors the exact expression of the parallel and perpendicular components of the susceptibility are given by³³ equations (2a) and (2b)

$$\chi_{\parallel} = N\beta^2 [g^2 \exp(J/4kT) + g^2 \exp(-J/4kT)] / 2kT \cosh(J/4kT) \quad (2a)$$

$$\chi_{\perp} = 2Ng_{\perp}^2 \beta^2 [\tanh(J/4kT)] / J \quad (2b)$$

where $g_{\pm} = \frac{1}{2}(g_{\parallel a} \pm g_{\parallel b})$ and $g_{\perp}^2 = \frac{1}{2}(g_{\perp a}^2 + g_{\perp b}^2)$.

The magnetic data of (5) and (8) were fitted to the magnetic susceptibility defined as $\chi = (\chi_{\parallel} + 2\chi_{\perp})/3$, in the ranges 1–10 K and 1–20 K respectively. The best fitted curves are illustrated in Figures 5(f) and (g). The resulting parameters are $g_{\parallel \text{Co}} = 6.7$, $g_{\parallel \text{Cu}} = 2.1$, $\bar{g}_{\perp} = 1.6$, $J = -1.4 \text{ cm}^{-1}$ for (5) and $g_{\parallel \text{Co a}} = 4.1$, $g_{\parallel \text{Co b}} = 10.0$, $\bar{g}_{\perp} = 0.45$, $J = -3.9 \text{ cm}^{-1}$ for (8).

Table 7. Magnetic characterization of bimetallic cdta dimers. The exchange strengths J are based on the J Hamiltonian described in the text. J Values have been multiplied by a scaling factor of $\frac{3}{5}$ for (9), (4), and (5) and by $\frac{9}{25}$ for (8) to account for the effective spin of Co^{II} .³¹ J Values of the bimetallic edta analogues are given in parentheses

Compd.	g_a	g_b	$-J/\text{cm}^{-1}$	Model
(1)	2.19	2.19	6.8 (5.8)	Heisenberg
(2)	2	2.15	2.2 (1.1)	Heisenberg
(3)	2	2.13	2.1 (0.3)	Heisenberg
(9)	2	5.13 (g_{\parallel}) 4.2 (g_{\perp})	2.1 (0.9)	Ising
(4)	7.0 (g_{\parallel}) 3.3 (g_{\perp})	2.10	8.8 (5.2)	Ising
(5)	6.7 (g_{\parallel}) 1.6 (g_{\perp})	2.1 (g_{\parallel})	0.8 (2.3)	Ising
(8)	4.1 (g_{\parallel}) 0.45 (g_{\perp})	10.0 (g_{\parallel})	1.4 (5.7)	Ising

Final remarks. The resulting magnetic parameters of the reported compounds are displayed in Table 7. In accordance with the type of bidentate bridging carboxylate group ($a-2-a$ or $a-2-s$ structural functions¹¹), the interactions are weak and comparable to the values found in the edta derivatives $[\text{M}(\text{OH}_2)_4][\text{M}'(\text{edta})\cdot 2\text{H}_2\text{O}]$.^{3-6,34} Thus, the same kind of variation in the exchange strengths is observed in both families, with couplings systematically stronger in the cdta series. The largest differences between J values have been shown by the Cu^{II} containing derivatives. This observation emphasises, once again, the greater sensitivity of this ion to small variations in the bridging angles. On the other hand, obtaining the same trend in the J values for the derivatives of the two ligands could justify the validity of the models which have been developed and used to approach the magnetic behaviour of the ferromagnetic edta chains, since for most of them only approximate solutions can be achieved.

Dealing with the exchange anisotropy of (9), (4), (5), and (8) a fully anisotropic Ising model could be questionable for describing these systems. In fact, in the analogous Co,Cu and Co,Co edta systems, anisotropies of $J_{\perp}/J_{\parallel} = 0.35$ and 0.22 have been estimated from specific heat data respectively.³⁵ Accordingly, an intermediate model should be more realistic in the present case. In any case, this kind of treatment, aside from increasing the number of adjustable parameters, could not improve the fit.

Finally, further experimental work (e.s.r. on diluted compounds and lower temperature magnetic measurements) is yet required in order to obtain accurate and independent determinations of the local parameters (g tensors and zero-field splittings).

Acknowledgements

We thank the Comisión Asesora de Investigación Científica y Técnica and Consejo Superior de Investigaciones Científicas for financial support and for a postdoctoral fellowship (to A. F.). We are grateful to Drs. R. Burriel and M. Drillon for making available the magnetic measurements.

References

- 1 R. L. Carlin, *Coord. Chem. Rev.*, 1987, **79**, 215 and refs. therein.
- 2 E. Escrivá, A. Fuertes, and D. Beltrán, *Transition Met. Chem.*, 1984, **9**, 184.

- 3 M. Drillon, E. Coronado, D. Beltrán, and R. Georges, *Chem. Phys.*, 1983, **79**, 449.
- 4 M. Drillon, E. Coronado, D. Beltrán, and R. Georges, *J. Appl. Phys.*, 1985, **57**, 3353.
- 5 M. Drillon, E. Coronado, D. Beltrán, J. Curely, R. Georges, P. R. Nugteren, L. J. de Jongh, and J. L. Genicon, *J. Magnetism Magn. Mater.*, 1986, **54**, 1507.
- 6 E. Coronado, M. Drillon, A. Fuertes, D. Beltrán, A. Mosset, and J. Galy, *J. Am. Chem. Soc.*, 1986, **108**, 900.
- 7 A. Fuertes, C. Miravittles, E. Escrivá, E. Martínez-Tamayo, and D. Beltrán, *Transition Met. Chem.*, 1985, **10**, 432.
- 8 A. Fuertes, E. Escrivá, M. C. Muñoz, J. Alamo, A. Beltrán-Porter, and D. Beltrán-Porter, *Transition Met. Chem.*, 1987, **12**, 62.
- 9 A. Fuertes, C. Miravittles, E. Escrivá, E. Coronado, and D. Beltrán, *J. Chem. Soc., Dalton Trans.*, 1986, 1795.
- 10 A. Fuertes, C. Miravittles, E. Molins, E. Escrivá, and D. Beltrán, *Acta Crystallogr., Sect. C*, 1986, **42**, 421.
- 11 A. Fuertes, C. Miravittles, E. Escrivá, E. Coronado, and D. Beltrán, *J. Chem. Soc., Dalton Trans.*, 1987, 1847.
- 12 A. Mosset, J. Galy, C. Muñoz-Roca, and D. Beltrán-Porter, *Z. Kristallogr.*, 1987, **181**, 83.
- 13 P. Main, S. J. Fiske, S. E. Hull, L. Lessinger, G. Germain, J. P. Declercq, and M. M. Woolfson, MULTAN 11/82, a system of computer programs for the automatic solution of crystal structures from X-ray diffraction data, Universities of York (England) and Louvain (Belgium), 1982.
- 14 G. M. Sheldrick, SHELX 76, Program for Crystal Structure Determination, Cambridge University, 1976.
- 15 'International Tables for X-Ray Crystallography,' Kynoch Press, Birmingham, 1974, vol. 1, pp. 72, 99.
- 16 P. Roberts and G. M. Sheldrick, XANADU, Program for Crystallographic Calculations, Cambridge University, 1975.
- 17 J. Burzlaff, V. Böhme, and M. Gomm, DISTAN, University of Erlangen, Federal Republic of Germany, 1977.
- 18 W. D. S. Motherwell and W. Clegg, PLUTO 78, Program for Plotting Molecular and Crystal Structures, Cambridge University, 1978.
- 19 H. A. Weakliem and J. L. Hoard, *J. Am. Chem. Soc.*, 1959, **81**, 549.
- 20 B. J. Hathaway, *Coord. Chem. Rev.*, 1983, **52**, 87.
- 21 B. J. Hathaway and D. E. Billing, *Coord. Chem. Rev.*, 1970, **5**, 143.
- 22 M. A. Porai-Koshits, A. I. Pozhidaev, and T. N. Polynova, *Zh. Strukt. Khim.*, 1974, **15**, 1117.
- 23 M. A. Porai-Koshits, *Zh. Strukt. Khim.*, 1980, **21**, 146.
- 24 A. N. Pozhidaev, Ya. M. Nesterova, T. N. Polynova, M. A. Porai-Koshits, and V. A. Logvinenko, *Zh. Strukt. Khim.*, 1977, **18**, 408.
- 25 M. G. Drew, *Prog. Inorg. Chem.*, 1977, **23**, 67.
- 26 M. D. Lind, J. L. Hoard, M. J. Hamor, and T. A. Hamor, *Inorg. Chem.*, 1964, **3**, 34.
- 27 G. H. Cohen and J. L. Hoard, *J. Am. Chem. Soc.*, 1966, **88**, 3228.
- 28 A. Fuertes, Ph.D. Thesis, Universidad de Valencia, 1986.
- 29 M. E. Lines, *J. Chem. Phys.*, 1971, **35**, 2977.
- 30 L. Banci, A. Bencini, C. Benelli, D. Gatteschi, and C. Zanchini, *Struct. Bonding (Berlin)*, 1982, **52**, 37.
- 31 E. Coronado, M. Drillon, D. Beltrán, and J. C. Bernier, *Inorg. Chem.*, 1984, **23**, 4000.
- 32 J. Curely, R. Georges, and M. Drillon, *Phys. Rev. B*, 1986, **33**, 6243.
- 33 E. Coronado, P. R. Nugteren, M. Drillon, D. Beltrán, and L. J. de Jongh, unpublished work.
- 34 E. Coronado, P. R. Nugteren, M. Drillon, D. Beltrán, L. J. de Jongh, and R. Georges, 'Organic and Inorganic Low-dimensional Crystal-line Materials,' eds. B. Delhaes and M. Drillon, N.A.T.O. ASI series, Plenum Press, New York, 1987.
- 35 E. Coronado, M. Drillon, P. R. Nugteren, L. J. de Jongh, and D. Beltrán, *J. Am. Chem. Soc.*, 1988, **110**, 3907.